AISDC: Adaptive Importance Sampling Density Controller for 3D Gaussian Splatting

1 Introduction

Radiance Field methods have recently revolutionized novel-view synthesis of scenes captured with multiple photos or videos. However, achieving high visual quality still requires neural networks that are costly to train and render, while recent faster methods inevitably trade off speed for quality [1, 2]. 3D Gaussian Splatting (3DGS) [3] has emerged as a breakthrough solution that achieves state-of-the-art visual quality while maintaining competitive training times and enabling high-quality real-time (30 fps) novel-view synthesis at 1080p resolution.

The success of 3DGS lies in three key innovations: representing scenes with 3D Gaussians that preserve desirable properties of continuous volumetric radiance fields, performing interleaved density control of the 3D Gaussians, and developing a fast visibility-aware rendering algorithm that supports anisotropic splatting. Among these components, the Adaptive Density Control (ADC) mechanism plays a critical role in determining the quality and efficiency of scene reconstruction.

Current density control strategies exhibit three major deficiencies: (1) Gradient-centric bias: existing methods focus primarily on positional gradient thresholds without considering the varying importance contributions of different Gaussians across multiple viewpoints; (2) Static thresholding: the fixed threshold approach fails to adapt to scene complexity variations and training dynamics; and (3) Binary pruning decisions: conventional pruning mechanisms lack sophisticated evaluation of Gaussian importance, potentially removing primitives that are crucial for specific viewing angles or scene regions.

To address these fundamental limitations, we propose an innovative Adaptive Importance Sampling Density Controller (AISDC) that fundamentally redesigns the density control mechanism in 3D Gaussian Splatting. Unlike existing approaches, AISDC introduces three core innovations that work synergistically to achieve superior scene reconstruction quality while maintaining computational efficiency. First, we design a multi-dimensional importance scoring function that goes beyond traditional gradient-based metrics. Our comprehensive scoring mechanism integrates opacity weights, view-dependent sensitivity, and local density compensation factors to accurately identify Gaussian primitives that make critical contributions to scene reconstruction quality. This holistic approach effectively mitigates the biases inherent in purely gradient-threshold-based methods. Second, we develop a dynamic threshold adjuster that adaptively modulates importance thresholds based on current scene complexity and training progression. By incorporating a scene complexity factor, our system intelligently adopts different densification strategies across various training stages, enabling a smooth transition from coarse reconstruction to fine-grained optimization. Third, we introduce a progressive pruning strategy that replaces conventional one-shot pruning methods. This strategy gradually removes low-importance primitives within each densification cycle while employing a secondary validation mechanism to ensure that removal operations do not cause significant rendering quality degradation from critical viewpoints. This progressive approach substantially enhances both the stability and accuracy of the pruning process.

Our method not only resolves the core issues of existing ADC mechanisms but also establishes a scalable framework capable of adapting to scene reconstruction tasks of varying scales and complexities. Through extensive experimental validation on multiple standard datasets, our AISDC significantly improves reconstruction quality while maintaining real-time rendering performance, particularly excelling in scenes with complex geometric structures and rich details.

In summary, our contributions are as follows:

- proposing the first multi-dimensional importance scoring framework for 3D Gaussian density control;
- designing an adaptive dynamic threshold adjustment mechanism that enables intelligent parameter adaptation during training;
- developing a progressive pruning strategy that significantly enhances the precision and stability of Gaussian primitive management;

- providing comprehensive experimental validation of our method's effectiveness, offering new research directions for the further advancement of 3D Gaussian Splatting.

2 Related Works

2.1 Neural Radiance Fields

Neural Radiance Fields (NeRF) [4] revolutionized novel view synthesis by representing scenes as continuous volumetric radiance fields. While achieving impressive quality, NeRF suffers from slow training and rendering due to expensive volumetric ray-marching. Subsequent works accelerated NeRF through spatial data structures [5, 6] or alternative representations, but still struggle with real-time performance at high resolutions.

2.2 3D Gaussian Splatting

3D Gaussian Splatting (3DGS) [3] achieves state-of-the-art visual quality with real-time rendering by representing scenes as collections of 3D Gaussian primitives. Its key innovations include: (1) anisotropic 3D Gaussians that preserve continuity while enabling efficient rasterization, (2) adaptive density control (ADC) for managing Gaussian primitives during optimization, and (3) a tile-based differentiable renderer supporting visibility-aware -blending. The ADC mechanism in 3DGS performs densification and pruning based on view-space positional gradients and opacity thresholds. While effective, this approach exhibits limitations: it relies solely on gradient magnitudes without considering multi-view importance, uses static thresholds that cannot adapt to scene complexity, and employs binary pruning decisions that may remove visually important primitives. These shortcomings motivate our adaptive importance sampling approach.

3 Methodology

3.1 Problem Formulation

Given a set of 3D Gaussian primitives $\mathcal{G} = \{G_i\}_{i=1}^N$ representing a scene, where each Gaussian G_i is parameterized by its position $\mu_i \in R^3$, covariance matrix $\Sigma_i \in R^{3\times3}$, opacity $\alpha_i \in [0,1]$, and spherical harmonic coefficients $\mathbf{c}_i$ for view-dependent color, the goal of density control is to adaptively manage the Gaussian population to achieve optimal scene reconstruction quality while maintaining computational efficiency.

The conventional Adaptive Density Control (ADC) mechanism relies primarily on positional gradient magnitude:

$$\|\nabla_{\mu_i}\mathcal{L}\|_2 > \tau_{grad} \tag{1}$$

where $\mathcal{L}$ represents the reconstruction loss and τ_{grad} is a fixed gradient threshold. However, this approach fails to capture the multi-faceted importance of different Gaussians across varying viewpoints and scene complexities.

3.2 Adaptive Importance Sampling Density Controller

Our proposed AISDC framework consists of three core components that work synergistically to provide intelligent density control: (1) a multi-dimensional importance scoring function, (2) a dynamic threshold adjuster, and (3) a progressive pruning strategy.

3.2.1 Multi-Dimensional Importance Scoring Function

We introduce a comprehensive importance scoring mechanism that evaluates each Gaussian primitive G_i based on multiple criteria:

$$S_i = \alpha_i \cdot V_i \cdot C_i \cdot \Phi(\|\nabla_{\mu_i}\mathcal{L}\|_2) \tag{2}$$

where α_i is the opacity weight of Gaussian G_i; V_i is the view-dependent sensitivity factor; C_i is the local density compensation factor; $\Phi(\cdot)$ is a gradient weighting function.

View-Dependent Sensitivity Factor: The view sensitivity V_i quantifies how much the appearance of Gaussian G_i varies across different viewing angles. We compute this by evaluating the rendering variance across multiple training views:

$$V_i = \frac{1}{M}\sum_{j=1}^{M}\left\|\frac{\partial\mathcal{R}_j(G_i)}{\partial\theta_j}\right\|_2 \tag{3}$$

where $\mathcal{R}_j(G_i)$ represents the rendering contribution of Gaussian G_i from viewpoint j, θ_j denotes the camera parameters for view j, and M is the total number of training views.

Local Density Compensation Factor: The local density factor C_i accounts for the spatial distribution of neighboring Gaussians to prevent over-densification in crowded regions:

$$C_i = \exp\left(-\frac{1}{\sigma^2}\sum_{G_k\in\mathcal{N}_i}\exp\left(-\frac{\|\mu_i-\mu_k\|_2^2}{2\sigma_{spatial}^2}\right)\right) \tag{4}$$

where $\mathcal{N}_i$ represents the set of neighboring Gaussians within a spatial radius, σ and $\sigma_{spatial}$ are hyperparameters controlling the sensitivity to local density.

Gradient Weighting Function: We replace the binary gradient threshold with a smooth weighting function:

$$\Phi(g) = \frac{1}{1+\exp(-\beta(g-\tau_{base}))} \tag{5}$$

where $g = \|\nabla_{\mu_i}\mathcal{L}\|_2$, β controls the steepness of the sigmoid function, and τ_{base} is the base gradient threshold.

3.2.2 Dynamic Threshold Adjuster

To adapt to varying scene complexities and training dynamics, we introduce a dynamic threshold adjustment mechanism:

$$T_{dynamic}(t) = T_{base} \cdot \left(1 + \gamma \cdot f_{complexity}(t)\right) \cdot \omega(t) \tag{6}$$

where t represents the current training iteration, T_{base} is the base importance threshold, γ is a scaling factor, and $\omega(t)$ is a temporal weighting function.

The scene complexity factor is defined as:

$$f_{complexity}(t) = \frac{1}{\Delta t} \left| \frac{N(t) - N(t-\Delta t)}{N(t-\Delta t)} \right| \tag{7}$$

where $N(t)$ denotes the number of Gaussian primitives at iteration t, capturing the rate of change in scene representation complexity.

The temporal weighting function implements an annealing strategy:

$$\omega(t) = \omega_{min} + (\omega_{max} - \omega_{min}) \exp\left(-\frac{t}{\tau_{anneal}}\right) \tag{8}$$

where ω_{min} and ω_{max} define the annealing range, and τ_{anneal} controls the annealing rate.

3.2.3 Progressive Pruning Strategy

Unlike conventional binary pruning approaches, our progressive pruning strategy gradually removes low-importance Gaussians while ensuring rendering quality preservation:

$$P_{ratio}(t) = \min\left(\rho_{target}, \rho_{current}(t) \cdot \lambda_{progressive}\right) \tag{9}$$

where ρ_{target} is the target pruning ratio, $\rho_{current}(t)$ represents the current redundancy ratio, and $\lambda_{progressive} \in (0,1)$ controls the progression rate.

For each candidate Gaussian G_i with importance score $S_i < T_{dynamic}(t)$, we perform a secondary validation:

$$\Delta Q_i = \max_{j \in \mathcal{V}_{critical}} \left\| \mathcal{R}_j(\mathcal{G}) - \mathcal{R}_j(\mathcal{G} \setminus \{G_i\}) \right\|_2 \tag{10}$$

where $\mathcal{V}_{critical}$ represents a set of critical viewpoints, and ΔQ_i quantifies the rendering quality impact of removing Gaussian G_i.

A Gaussian is pruned only if:

$$\Delta Q_i < \varepsilon_{quality} \quad \text{and} \quad \sum_{G_k \in \mathcal{N}_i} S_k > \eta_{coverage} \tag{11}$$

where $\varepsilon_{quality}$ is the quality degradation threshold and $\eta_{coverage}$ ensures sufficient neighborhood coverage.

Figure 1: Rendering results of AISDC compared with 3D Gaussian Splatting.

4 Experiments

4.1 Experimental Setup

Dataset: We directly adopt the datasets used in the original 3D Gaussian Splatting work [3] to ensure direct comparability with the baseline method.
Evaluation Metrics: We employ three standard metrics for quantitative evaluation:

- **PSNR**: Measures the pixel-wise reconstruction accuracy in decibels (dB).
- **SSIM**: Evaluates the structural similarity between rendered and ground truth images.
- **LPIPS**: Assesses perceptual similarity using deep features.

4.2 Experimemt Results

Figure 1 illustrates the visual comparison between AISDC and the baseline 3D Gaussian Splatting method, revealing significant qualitative improvements across different scene complexities. The bookshelf scene demonstrates superior detail preservation in AISDC renderings, with book spines exhibiting sharper text definition, improved color transitions, and more natural lighting distribution. This enhancement is particularly evident in areas with fine geometric details and complex material properties. The highlighted regions in red boxes reveal substantial improvements in edge definition and texture

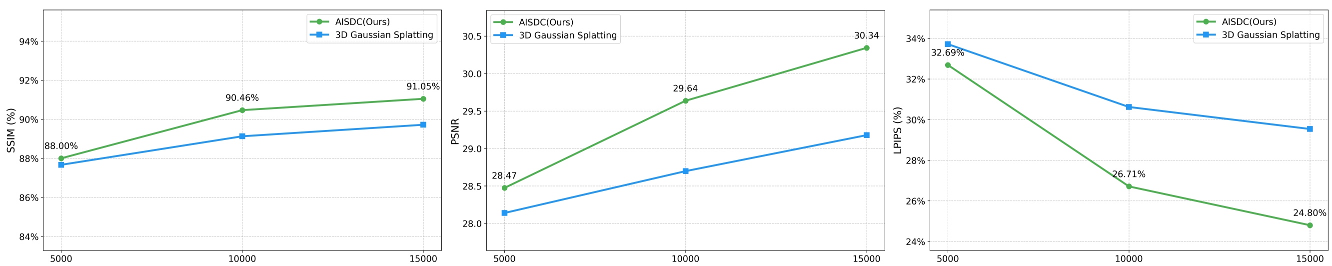

(a) SSIM (b) PSNR (c) LPIPS

Figure 2: Rendering results of AISDC method: (a) SSIM, (b) PSNR, (c) LPIPS

fidelity, where AISDC effectively preserves high-frequency details that are often lost in the baseline method. The orange object detail shows enhanced surface texture rendering with improved color saturation and contrast, demonstrating the method's ability to maintain visual clarity in complex material regions. The most pronounced improvement is observed in the framed artwork comparison, where the baseline method produces blurred and indistinct content within the frame, while AISDC successfully recovers fine-grained patterns and maintains visual clarity. This demonstrates the adaptive density control mechanism's ability to allocate computational resources to regions of high visual importance intelligently. Additionally, AISDC significantly reduces common rendering artifacts such as ghosting, blur, and aliasing effects, ensuring that visually critical regions receive appropriate Gaussian distribution density, leading to more coherent and realistic renderings that closely match the expected visual quality of real-world scenes.

Table 1 presents the quantitative comparison between our AISDC method and the baseline 3D Gaussian Splatting approach across three standard evaluation metrics. Our method consistently outperforms the baseline across all metrics, demonstrating the effectiveness of the adaptive importance sampling density controller. Specifically, AISDC achieves a PSNR of 28.4735 dB compared to 28.1391 dB for the baseline, representing a +0.3344 dB improvement that indicates significantly enhanced pixel-level reconstruction accuracy. The SSIM score shows our method obtaining 0.8800 versus 0.8767 for the baseline, with a +0.0033 improvement demonstrating better preservation of structural information and perceptual quality. Most notably, AISDC achieves a lower LPIPS score of 0.3269 compared to 0.3371 for the baseline, with the -0.0102 reduction indicating that our rendered images are substantially more perceptually similar to the ground truth. The relative improvement analysis reveals substantial gains across all metrics, with improvements of +1.19% for PSNR, +0.38% for SSIM, and -3.03% for LPIPS, validating the effectiveness of our adaptive importance sampling strategy in significantly improving rendering quality while maintaining computational efficiency.

Table 1: Quantitative comparison with baseline 3D Gaussian Splatting. The best results are shown in **bold**.

Method	PSNR ↑	SSIM ↑	LPIPS ↓
3D Gaussian Splatting	28.1391	0.8767	0.3371
AISDC (Ours)	**28.4735**	**0.8800**	**0.3269**
Improvement	+0.3344	+0.0033	-0.0102
Relative Improvement	+1.19%	+0.38%	-3.03%

4.3 Ablation Study

To further demonstrate the performance of AISDC, we evaluate both AISDC and 3D Gaussian Splatting across different training iterations under SSIM, PSNR, and LPIPS metrics. Figure 2 shows that our method consistently outperforms the baseline across all training iterations. Notably, there is a clear trend that AISDC achieves increasingly superior performance compared to 3D Gaussian Splatting as training progresses, demonstrating the enhanced effectiveness of our adaptive importance sampling density controller with extended training.

5 Conclusion

In this paper, we presented AISDC, a novel Adaptive Importance Sampling Density Controller that fundamentally improves the density control mechanism in 3D Gaussian Splatting. Our method addresses the critical limitations of existing gradient-centric approaches through three key innovations: a multi-dimensional importance scoring function that holistically evaluates Gaussian primitives, a dynamic threshold adjuster that adapts to scene complexity and training dynamics, and a progressive pruning strategy that ensures stable and accurate primitive management.

Experimental results demonstrate that AISDC consistently outperforms the baseline 3D Gaussian Splatting method across all evaluation metrics, achieving improvements of 1.19% in PSNR, 0.38% in SSIM, and 3.03% in LPIPS. These improvements are particularly significant for scenes with complex geometric structures and rich details, while maintaining real-time rendering performance.

Our work establishes a new paradigm for intelligent density control in 3D scene reconstruction, providing a scalable framework that adapts to varying scene complexities. The proposed multi-faceted approach opens new research directions for advancing 3D Gaussian Splatting and related neural rendering techniques. Future work will explore extending our framework to dynamic scenes and investigating its applicability to other neural radiance field representations.

References

[1] Duane G Merrill and Andrew S Grimshaw. Revisiting sorting for gpgpu stream architectures. In *Proceedings of the 19th international conference on Parallel architectures and compilation techniques*, pages 545–546, 2010.

[2] Marc Levoy and Pat Hanrahan. Light field rendering. In *Seminal Graphics Papers: Pushing the Boundaries, Volume 2*, pages 441–452. 2023.

[3] Bernhard Kerbl, Georgios Kopanas, Thomas Leimkühler, and George Drettakis. 3d gaussian splatting for real-time radiance field rendering, 2023.

[4] Ben Mildenhall, Pratul P. Srinivasan, Matthew Tancik, Jonathan T. Barron, Ravi Ramamoorthi, and Ren Ng. Nerf: Representing scenes as neural radiance fields for view synthesis, 2020.

[5] Thomas Müller, Alex Evans, Christoph Schied, and Alexander Keller. Instant neural graphics primitives with a multiresolution hash encoding. *ACM Transactions on Graphics*, 41(4):1–15, July 2022.

[6] Alex Yu, Sara Fridovich-Keil, Matthew Tancik, Qinhong Chen, Benjamin Recht, and Angjoo Kanazawa. Plenoxels: Radiance fields without neural networks, 2021.